Draft version September 7, 2017
Preprint typeset using LaTeX style emulateapj v. 12/16/11

THE INTERIOR ANGULAR MOMENTUM OF CORE HYDROGEN BURNING STARS FROM GRAVITY-MODE OSCILLATIONS

C. Aerts[1,2,3], T. Van Reeth[1,3], A. Tkachenko[1]

Draft version September 7, 2017

ABSTRACT

A major uncertainty in the theory of stellar evolution is the angular momentum distribution inside stars and its change during stellar life. We compose a sample of 67 stars in the core-hydrogen burning phase with a $\log g$ value from high-resolution spectroscopy, as well as an asteroseismic estimate of the near-core rotation rate derived from gravity-mode oscillations detected in space photometry. This assembly includes 8 B-type stars and 59 AF-type stars, covering a mass range from 1.4 to 5 $M_\odot$, i.e., it concerns intermediate-mass stars born with a well-developed convective core. The sample covers projected surface rotation velocities $v \sin i \in [9, 242]\,\mathrm{km\,s^{-1}}$ and core rotation rates up to 26μHz, which corresponds to 50% of the critical rotation frequency. We find deviations from rigid rotation to be moderate in the single stars of this sample. We place the near-core rotation rates in an evolutionary context and find that the core rotation must drop drastically before or during the short phase between the end of the core-hydrogen burning and the onset of core-helium burning. We compute the spin parameter, which is the ratio of twice the rotation rate to the mode frequency (also known as the inverse Rossby number), for 1682 gravity modes and find the majority (95%) to occur in the sub-inertial regime. The ten stars with Rossby modes have spin parameters between 14 and 30, while the gravito-inertial modes cover the range from 1 to 15.

Subject headings: asteroseismology – stars: evolution – stars: massive – stars: oscillations (including pulsations) – stars: rotation – waves

1. INTRODUCTION

Rotation has a significant impact on the life of a star (e.g., Maeder 2009). It induces a multitude of hydrodynamical processes that affect stellar structure but have remained poorly calibrated by data. While surface abundances and surface rotation give some constraints for stellar models, one needs calibrations of the interior rotation and chemical mixing profiles of stars to evaluate the theoretical concepts that have been developed to describe transport phenomena and their interplay (e.g., Heger et al. 2000; Meynet et al. 2013). Here, we are concerned with the interior rotation rate of stars in the core-hydrogen burning phase of their life (aka the main sequence).

Asteroseismology based on long-term high-precision monitoring of nonradial oscillations is the best way to deduce the interior rotation of stars, following the case of helioseismology (e.g. Thompson et al. 2003). Early estimates of the interior rotation of main sequence stars were achieved from rotational splitting of a few pressure modes in β Cep stars from ground-based data (Aerts et al. 2003; Pamyatnykh et al. 2004; Briquet et al. 2007). However, it concerned only very rough estimates of the ratio of the near-core to envelope rotation rates, with values from 1 to ~ 4 for three stars with a mass between 8 and 10 $M_\odot$ (Aerts 2008, for a summary).

A major breakthrough in the derivation of interior rotation rates was achieved thanks to the NASA *Kepler* mission, once it had delivered light curves with a duration longer than two years. The early and so far majority of interior rotation rates were obtained from the rotational splitting of dipole mixed modes in low- and intermediate-mass evolved stars (subgiants and red giants with a mass between 0.8 and 3.3 $M_\odot$; Beck et al. 2012; Mosser et al. 2012; Deheuvels et al. 2012, 2014, 2015). These seismic results constituted an unanticipated result, since the cyclic rotation frequency $\Omega/2\pi$ of the stellar core (denoted as $\Omega_{\rm core}$ hereafter) of these evolved stars turned out to be two orders of magnitude lower than theoretical predictions. This pointed to stronger coupling between the stellar core and envelope during and/or after the main sequence, irrespective of the star having undergone a helium flash or not. This major shortcoming of the theory of angular momentum transport remains unsolved (e.g. Tayar & Pinsonneault 2013; Cantiello et al. 2014; Eggenberger et al. 2017). In Sect. 2, we shed new light on this topic by considering the interior rotation rates derived so far from *Kepler* and BRITE photometry of red-giant progenitors, i.e., intermediate-mass gravity-mode pulsators on the main sequence.

In Sect. 3, we provide the observational information to evaluate the assumptions made in the theory of angular momentum transport by waves. A promising physical ingredient that can explain the observed behavior of the core-to-surface rotation of main sequence stars is the transport of angular momentum by low-frequency internal gravity waves created at the interface between the convective core and the radiative envelope, observed from space photometry (Aerts & Rogers 2015; Rogers 2015). The theory of the interaction between such waves and (differential) rotation inside stars requires proper treatment of the various forces at play. Based on our findings

[1] Institute of Astronomy, KU Leuven, Celestijnenlaan 200D, B-3001 Leuven, Belgium
[2] Department of Astrophysics, IMAPP, Radboud University Nijmegen, P.O. Box 9010, 6500 GL Nijmegen, The Netherlands
[3] Kavli Institute for Theoretical Physics, University of California, Santa Barbara, CA 93106, USA

for the rotation, we provide the spin parameters (inverse Rossby numbers) of the gravity modes as input for angular momentum computations. We end the paper with a discussion in Sect. 4.

2. CORE ROTATION FROM GRAVITY-MODE OSCILLATIONS

Gravity-mode oscillations of main sequence stars have periods from 0.5 to 3 d (e.g., Aerts et al. 2010, Chapter 2). Recent space photometry revealed period spacing patterns of such modes in B-, A- and F-type stars covering the entire main sequence (e.g. Degroote et al. 2010; Pápics et al. 2014; Kurtz et al. 2014; Saio et al. 2015; Van Reeth et al. 2015; Murphy et al. 2016; Ouazzani et al. 2017; Pápics et al. 2017; Zwintz et al. 2017), just as predicted by theory (Miglio et al. 2008; Bouabid et al. 2013). Such modes have their dominant mode energy in the near-core region of the star and are therefore excellent probes of the chemical gradient left behind during the main sequence shrinkage of the convective core. The detected gravity modes have rotational kernels that are typically 5 to 10 times larger in a narrow near-core region than in the extended radiative envelope (e.g., Triana et al. 2015; Van Reeth et al. 2016, their Figs 2).

For stars that reveal both gravity and pressure modes with rotational splitting, derivation of $\Omega_{\rm core}$ and $\Omega_{\rm env}$ is possible in an almost model-independent way. This was first achieved by Kurtz et al. (2014) for the A-type *Kepler* target KIC 11145123 and soon followed by Saio et al. (2015) for the F-type star KIC 9244992. More so-called hybrid pulsators with rotational splitting in both types of modes have been found meanwhile.

The majority of intermediate-mass gravity-mode pulsators found in the *Kepler* data reveal quantitative information on the near-core rotation but not on the envelope rotation. As derived by Van Reeth et al. (2016) and Ouazzani et al. (2017), the slope of the period spacing pattern of prograde, zonal, or retrograde modes of consecutive radial order delivers a direct probe of $\Omega_{\rm core}$, even in the absence of rotational splitting. A value of $\Omega_{\rm env}$ can be deduced from rotational splitting of pressure modes. In the absence of identified pressure modes, the surface rotation can still be derived with high precision from the detection of rotational modulation when this phenomenon occurs together with gravity modes in the light curves. Otherwise, only a lower limit for $\Omega_{\rm env}$ can be deduced from a spectroscopic measurement of the projected surface rotation velocity $\Omega_{\rm env} R \sin i$ (Murphy et al. 2016; Van Reeth et al. 2016). This can be achieved by adopting a reasonable value for the stellar radius while paying attention to line-profile broadening induced by all the tangential velocity fields due to gravity modes (Aerts et al. 2014b).

Figure 1 includes 67 main sequence stars from Kurtz et al. (2014); Saio et al. (2015); Triana et al. (2015); Moravveji et al. (2016); Murphy et al. (2016); Van Reeth et al. (2016); Schmid & Aerts (2016); Ouazzani et al. (2017); Pápics et al. (2017); Sowicka et al. (2017); Kallinger et al. (2017), and Guo et al. (submitted), covering spectral types from mid B to early F. All these studies rely on *Kepler* or BRITE space photometry. Their gravity modes revealed $\Omega_{\rm core}$ through asteroseismology and their $\log g$ resulted from high-resolution spectroscopy (except for the four stars in Ouazzani et al. (2017), for which we took $\log g$ from the *Kepler* input catalogue and estimated its error from Van Reeth et al. (2015), their Fig. 2). For 18 of the stars, the surface rotation rate is also available, either from asteroseismology of pressure modes or from rotational modulation. Twelve main sequence stars are member of a spectroscopic binary.

The 59 green stars in Fig. 1 cover $1.4\,{\rm M}_\odot$ <M< $2.0\,{\rm M}_\odot$ and $v \sin i \in [9, 170]\,{\rm km\,s^{-1}}$. According to Zorec & Royer (2012), stars in this mass range rotate on average with $v \sin i = 148\,{\rm km\,s^{-1}}$, with a dispersion of $54\,{\rm km\,s^{-1}}$. Given that none of the $v \sin i$ studies of large ensembles take into account pulsational line broadening, while this overestimates $v \sin i$ (Aerts et al. 2014b), our sample of AF stars is representative in terms of surface rotation for this mass range. On the other hand, our sample contains only 8 B stars with a mass in $3\,{\rm M}_\odot$ <M< $5\,{\rm M}_\odot$. While they cover a broad range of $v \sin i \in [18, 242]\,{\rm km\,s^{-1}}$, they are not representative of the bimodal distribution for this mass range (Table 4 in Zorec & Royer 2012). For both the B and AF stars in Fig. 1, the highest core rotation frequency corresponds to $\sim$ 50% of the critical value in the Roche formalism. At present, core rotation from gravity modes for stars rotating faster than half critical are not available from seismic modeling due to lack of mode identification.

We deduce from Fig. 1 that the deviation from rigid rotation in our sample of 67 stars is low to moderate, pointing to strong core-to-envelope coupling during core hydrogen burning, irrespective of the value of the rotation rate. Unfortunately, the errors for the spectroscopic $\log g$ are too large for this quantity to serve as a proxy of the evolutionary stage of the sample stars. Ideally, we want to use the central hydrogen fraction X_c from seismic modeling on the $x-$axis rather than $\log g$. At present this time-consuming task was only done for two B stars, revealing both to be in the first part of the main sequence with $X_c = 0.63 \pm 0.01$ and 0.50 ± 0.01, in agreement with the spectroscopic $\log g$ of the former being 0.2 dex higher than the one of the latter (Moravveji et al. 2015, 2016). For five of the eight F stars in the inset in Fig. 1, a seismic estimate of the evolutionary stage is available from comparison of the morphology of the gravity-mode period spacings: $X_c \in [0.01, 0.22]$.

Differences in the core-to-surface rotation, even if moderate, are significant for several stars in Fig. 1. Both faster cores than surfaces and vice versa occur. Large nonrigidity occurs in some close binaries, where tidal forces are active. Even though we cannot pinpoint X_c values for all stars at present, the results in Fig. 1 require an angular momentum redistribution mechanism that can explain the diversity of the measured core-to-envelope rotation during core hydrogen burning. One such mechanism is discussed in the following section.

To interpret the results in Fig. 1 in a more global evolutionary context, we also show the core and surface rotation rates of successors of these 67 stars, i.e., red giants on the RGB (red), in the red clump (gray), and in the secondary clump (orange), limiting to the 152 stars with masses above $1.4\,{\rm M}_\odot$ from Mosser et al. (2012); Deheuvels et al. (2015) and one binary from Beck et al. (2014). For all these evolved stars, the gravity in the

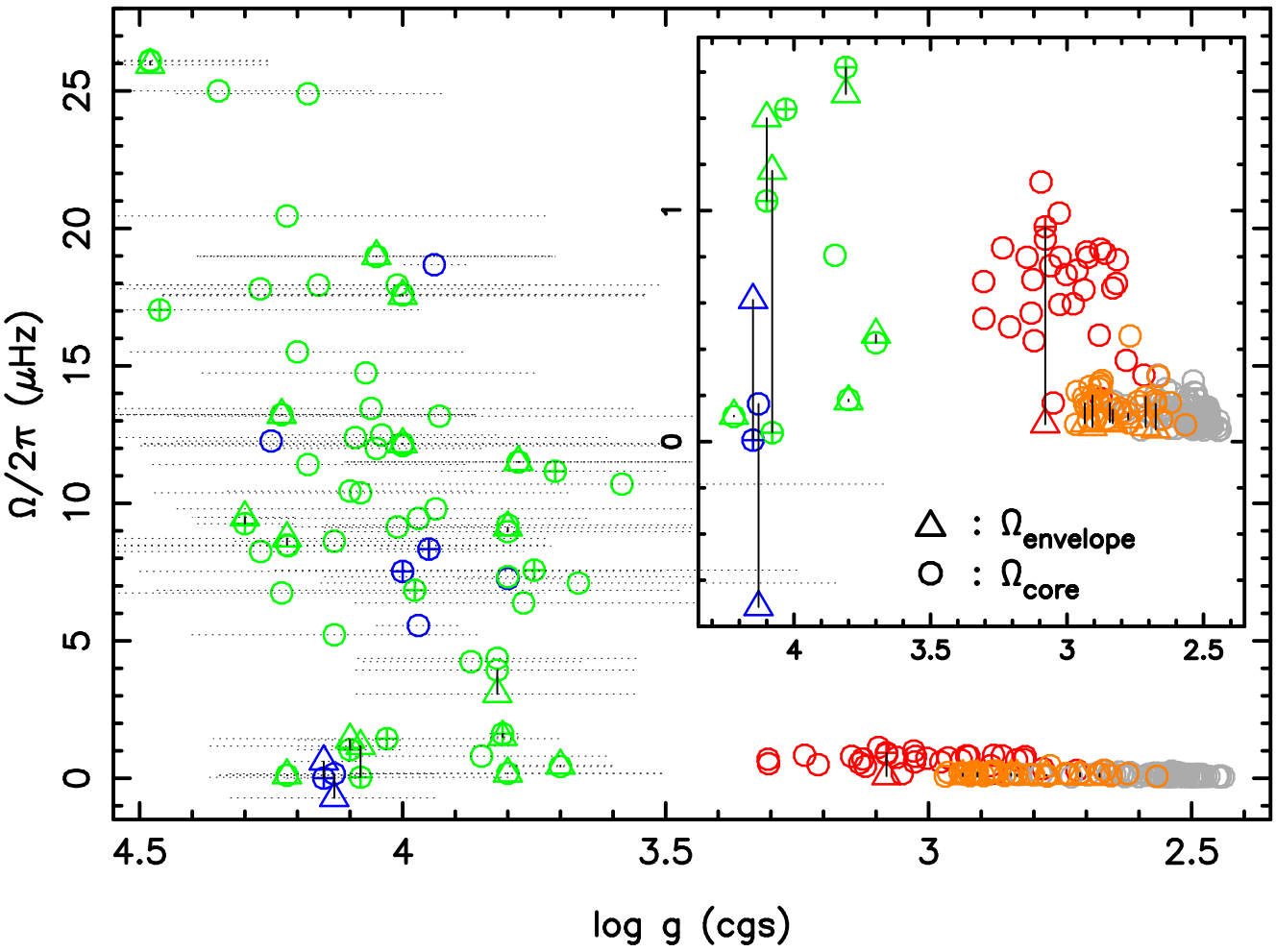

FIG. 1.— Core rotation rates (circles) as a function of spectroscopically-derived gravity for core-hydrogen burning stars with a mass between 1.4 and 2.0 $M_\odot$ (green) and 3 to $\sim$ 5 $M_\odot$ (blue) derived from dipole prograde gravito-inertial modes in main sequence stars. Surface rotation rates (triangles) are deduced from pressure modes or from rotational modulation. Errors on the rotation rates are smaller than the symbol size, while the errors on the gravity are indicated by dotted lines. Asteroseismically derived rotation rates and gravities for evolved stars with solar-like oscillations in the mass range 1.4 $M_\odot$ <M< 3.3 $M_\odot$ have been added (errors smaller than symbol sizes for both quantities): RGB stars (red), red clump stars (gray) and secondary clump stars (orange). Binary components are indicated with an extra + sign inside the circles. The errors of log g have been omitted in the zoomed window for clarity.

figure is derived from scaling relations of solar-like oscillations (errors are smaller than the symbol size; B. Mosser kindly made the masses and radii of the stars in Mosser et al. (2012) available to us). As argued by Mosser et al. (2014), stars born with M> 2.1 $M_\odot$ avoid a helium flash after the hydrogen shell burning. Their core contraction during hydrogen shell burning occurs on a short timescale (the so-called Hertzsprung gap) and the onset of core helium burning happens quietly in non-degenerate matter. These stars are hard to catch in their shell burning phase but reveal themselves as secondary clump stars (mass range up to 3.3 $M_\odot$ in Fig. 1). On the other hand, the successors of the stars born with 1.4 $M_\odot$ <M< 2.1 $M_\odot$ can readily be observed while burning hydrogen in a shell surrounding their helium core and start helium burning violently in degenerate matter.

The importance of the stellar mass and the occurrence (or not) of a convective core and/or $\mu-$gradient zone for the evolution of the angular momentum was already emphasized by Tayar & Pinsonneault (2013) and Eggenberger et al. (2017). This becomes even more prominent from our sample of intermediate-mass gravity-mode pulsators: efficient slow-down of the stellar core happens already on the main sequence for stars with a convective core. The three slowest rotators among the B stars have masses between 3.0 and 3.3 $M_\odot$ and are thus progenitors of the most massive orange stars; two of these are mid main sequence while the one with the counter-rotating envelope is young with $X_c = 0.63$.

3. ANGULAR MOMENTUM TRANSPORT BY WAVES

2D simulations of angular momentum transport by internal gravity waves of a 3 $M_\odot$ star at birth are able to explain the observed core-to-envelope rotation in Fig. 1 in a qualitative sense (Rogers 2015). Such simulations are computationally too demanding to be coupled to stellar evolution computations. The latter thus must resort to analytical treatments of angular momentum transport. These rely on approximations (e.g., Mathis 2011, for a didactic chapter).

Observed sub- and super-inertial waves can only propagate in a mode cavity set by the Brüntt-Väisälä frequency N. Nonlinear wave interactions for the low-frequency

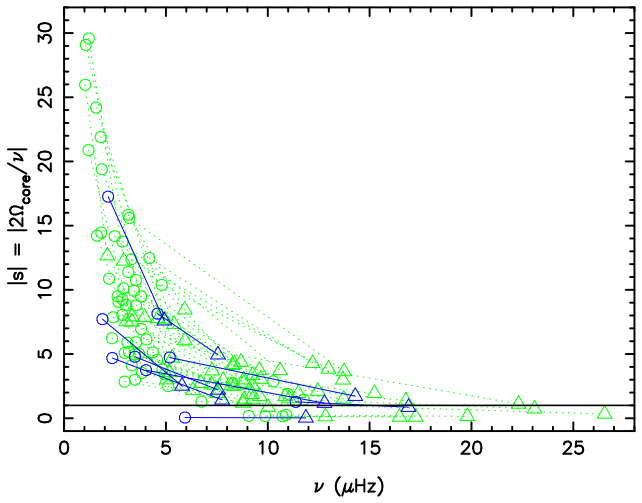

FIG. 2.— Spin parameters for 47 main sequence stars in Fig. 1 for which we identified the mode wavenumbers (same color convention). For each star, the range in frequencies of detected mode series of consecutive radial order is indicated by a line, from the circle that represents the mode with the lowest frequency in the corotating frame to the triangle representing the mode with the highest frequency. For all the F-type stars with $|s| > 15$, the high spin parameters are caused by low-frequency retrograde Rossby modes.

regime can at first instance be ignored because the mode frequencies (denoted as ν) fulfill $\nu < N$. The displacement vector of the observed coherent heat-driven gravity modes excited in the partial ionization zone of iron-like elements are dominantly horizontal. Indeed, multicolor photometry and high-precision line-profile variations in spectroscopy reveal a typical ratio of 10 to 100 between the horizontal and vertical component of the displacement vector of the gravity modes (De Cat & Aerts 2002). There is no reason why this would not be the case for convectively driven internal gravity waves. This property simplifies the theoretical treatment of the wave transport (Mathis 2011). The adiabatic and Cowling approximations are appropriate to describe the low-frequency gravity waves in the near-core region of our sample stars.

Ignoring the Lorentz and tidal forces, this brings us to the key parameter to evaluate the approximations that can or cannot be made in the treatment of the angular momentum transport by waves: the interior rotation frequency of the star with respect to the wave frequencies. For the stars on the main sequence indicated in blue and green in Fig. 1, we provide an estimate of the importance of the Coriolis force for their transport of angular momentum. This importance is expressed by the spin parameter, also known as the inverse of the Rossby number and defined here as $s = 2\,\Omega_{\rm core}/\nu$, where ν is the cyclic frequency of the gravity wave under study in a reference frame of the star corotating with $\Omega_{\rm core}$. Defining a corotating reference frame is not obvious in the case of non-rigid rotation; we choose to define s with respect to the value of $\Omega(r)/2\pi$ that is most robustly determined. Following the properties of the rotational kernels of the gravity modes, this is the value in the near-core μ-gradient region (Triana et al. 2015; Van Reeth et al. 2016).

In Fig. 2 we show the computed spin parameters based on the asteroseismic $\Omega_{\rm core}$ and on the frequencies of the identified gravity-mode series with consecutive radial order for the 7 B-type stars in Pápics et al. (2014, 2015, 2017) and 40 F-type stars in Van Reeth et al. (2015), all of which are included in Fig. 1. For each star, we connect the lowest- and highest-frequency mode (in the corotating frame) to visualize the range of s for each series in each star and compare it to a Rossby number of 1 (horizontal black line). Figure 2 represents 1682 modes in these 47 stars, all of which have been detected and identified from 4-year *Kepler* space photometry. We find that most of the stars have gravito-inertial modes rather than pure gravity modes: 1607 modes have frequencies in the sub-inertial regime. Among the detected modes are 273 (17%) retrograde Rossby modes occuring in 10 F-type stars in the sample. The slowest rotators reveal 75 (i.e., $< 5\%$) pure gravity modes in the super-inertial regime. About 12% of the modes in the 7 B stars and 4% of the modes in the 40 AF stars occur in the super-inertial regime.

We conclude that only the modes in the slowest rotators fulfil the formal mathematical condition on the spin parameter to apply the so-called Traditional Approximation (TA) for the Coriolis force (Townsend 2003; Mathis 2011). The detected Rossby modes have by far the highest spin parameters, covering $s \in [14, 30]$, while the gravito-inertial modes have $s \in [1, 15]$. We point out that the core rotation rates in Fig. 1 were obtained by adopting the TA and assuming rigid rotation for the observed gravito-inertial modes of the stars. The assumption of rigidity is not a drawback, because these modes have by far their largest mode energy in the near-core region while the mode kernels and mass distribution in the stellar envelope hardly contribute to the core rotation values (Figs 12 and 2 in Kurtz et al. 2014; Van Reeth et al. 2016, respectively). On the other hand, it was shown by Ouazzani et al. (2017, Fig. 1), who considered both 1D and 2D treatments of the modes for static equilibrium models, that the TA still provides a good approximation in the case of zonal and prograde gravito-inertial modes for the frequency regimes and spin parameters treated here and used to derive Fig. 1. However, the TA is less justified for the 20 retrograde gravito-inertial modes among the 1607 sub-inertial modes. Modelling the 293 retrograde gravito-inertial and Rossby modes will benefit from a 2D non-perturbative treatment of the rotation as developed by Ouazzani et al. (2012).

4. DISCUSSION

An important aspect to consider along with simulations of angular momentum transport by internal gravity waves is the chemical mixing induced by these waves and its comparison with mixing prescriptions adopted in 1D stellar evolution codes. Hints that pulsational mixing might be dominant over rotational mixing were found from a sample of pulsating magnetic and non-magnetic OB-type stars (Aerts et al. 2014a). A quantitative evaluation of the level of mixing in the near-core region and in the radiative envelope can be obtained from gravity-mode asteroseismology (e.g., Moravveji et al. 2015, 2016). This opens new perspectives to include seismically calibrated prescriptions for mixing and angular momentum transport based on multi-D numerical simulations of waves in stellar evolution computations. First attempts to compute chemical mixing due to gravity waves look promising when com-

pared with asteroseismic results (Rogers & McElwaine 2017).

More gravity-mode pulsators than those treated here are under study, but they either have too few unambiguously identified modes to derive $\Omega_{\rm core}$ (e.g., Zwintz et al. 2017) or they have not been observed in spectroscopy to derive their $v \sin i$ and $\log g$ (e.g., Ouazzani et al. 2017). Including all those with identified modes but without a spectroscopic $\log g$ in Fig. 1 requires forward modeling to derive a seismic X_c and $\log g$. Progress to populate Fig. 1 more densely from deeper exploitation of the *Kepler* and BRITE data and to transform this figure into a true "evolutionary" diagram is expected in the near future.

Unfortunately, we currently lack $\Omega_{\rm core}$ from gravity modes for stars born with $> 5\,M_\odot$, and in particular of core-collapse supernova progenitors. A major breakthrough is expected from large samples of OB-type stars in the Milky Way and in the Large Magellanic Cloud to be observed during almost one year with the TESS mission (TESS Southern CVZ; Ricker et al. 2016, launch in 2018) and for the long pointings of the PLATO mission (Rauer et al. 2014, launch foreseen in 2026). Only after deducing the interior rotation of single and binary OB-type stars from asteroseismology covering the hydrogen and helium core and shell burning stages will we be able to understand angular momentum evolution and confront it with the one of white dwarfs and neutron stars.

CA and TVR are grateful for the kind hospitality and opportunity to perform part of this research at the Kavli Institute of Theoretical Physics, University of California at Santa Barbara, USA. The research leading to these results has received funding from the European Research Council (ERC) under the European Union's Horizon 2020 research and innovation programme (grant agreement N°670519: MAMSIE), from the Research Foundation Flanders (FWO, grant agreements G.0B69.13 and V4.272.17N) and from the National Science Foundation of the United States under Grant NSF PHY11–25915.

REFERENCES

Aerts, C. 2008, in IAU Symposium, Vol. 250, Massive Stars as Cosmic Engines, ed. F. Bresolin, P. A. Crowther, & J. Puls, 237–244
Aerts, C., Christensen-Dalsgaard, J., & Kurtz, D. W. 2010, Asteroseismology, Astronomy and Astrophsyics Library, Springer Berlin Heidelberg
Aerts, C., Molenberghs, G., Kenward, M. G., & Neiner, C. 2014a, ApJ, 781, 88
Aerts, C. & Rogers, T. M. 2015, ApJ, 806, L33
Aerts, C., Simón-Díaz, S., Groot, P. J., & Degroote, P. 2014b, A&A, 569, A118
Aerts, C., Thoul, A., Daszyńska, J., et al. 2003, Science, 300, 1926
Beck, P. G., Hambleton, K., Vos, J., et al. 2014, A&A, 564, A36
Beck, P. G., Montalban, J., Kallinger, T., et al. 2012, Nature, 481, 55
Bouabid, M.-P., Dupret, M.-A., Salmon, S., et al. 2013, MNRAS, 429, 2500
Briquet, M., Morel, T., Thoul, A., et al. 2007, MNRAS, 381, 1482
Cantiello, M., Mankovich, C., Bildsten, L., Christensen-Dalsgaard, J., & Paxton, B. 2014, ApJ, 788, 93
De Cat, P. & Aerts, C. 2002, A&A, 393, 965
Degroote, P., Aerts, C., Baglin, A., et al. 2010, Nature, 464, 259
Deheuvels, S., Ballot, J., Beck, P. G., et al. 2015, A&A, 580, A96
Deheuvels, S., Doğan, G., Goupil, M. J., et al. 2014, A&A, 564, A27
Deheuvels, S., García, R. A., Chaplin, W. J., et al. 2012, ApJ, 756, 19
Eggenberger, P., Lagarde, N., Miglio, A., et al. 2017, A&A, 599, A18
Heger, A., Langer, N., & Woosley, S. E. 2000, ApJ, 528, 368
Kallinger, T., Weiss, W. W., Beck, P. G., et al. 2017, A&A, 603, A13
Kurtz, D. W., Saio, H., Takata, M., et al. 2014, MNRAS, 444, 102
Maeder, A. 2009, Physics, Formation and Evolution of Rotating Stars, Astronomy and Astrophysics Library, Springer Berlin Heidelberg
Mathis, S. 2011, in Lecture Notes in Physics, Berlin Springer Verlag, ed. J.-P. Rozelot & C. Neiner, Vol. 832, 275
Meynet, G., Ekstrom, S., Maeder, A., et al. 2013, in Lecture Notes in Physics, Berlin Springer Verlag, ed. M. Goupil, K. Belkacem, C. Neiner, F. Lignières, & J. J. Green, Vol. 865, 3
Miglio, A., Montalbán, J., Noels, A., & Eggenberger, P. 2008, MNRAS, 386, 1487
Moravveji, E., Aerts, C., Pápics, P. I., Triana, S. A., & Vandoren, B. 2015, A&A, 580, A27
Moravveji, E., Townsend, R. H. D., Aerts, C., & Mathis, S. 2016, ApJ, 823, 130
Mosser, B., Benomar, O., Belkacem, K., et al. 2014, A&A, 572, L5
Mosser, B., Goupil, M. J., Belkacem, K., et al. 2012, A&A, 548, A10
Murphy, S. J., Fossati, L., Bedding, T. R., et al. 2016, MNRAS, 459, 1201
Ouazzani, R.-M., Dupret, M.-A., & Reese, D. R. 2012, A&A, 547, A75
Ouazzani, R.-M., Salmon, S. J. A. J., Antoci, V., et al. 2017, MNRAS, 465, 2294
Pamyatnykh, A. A., Handler, G., & Dziembowski, W. A. 2004, MNRAS, 350, 1022
Pápics, P. I., Moravveji, E., Aerts, C., et al. 2014, A&A, 570, A8
Pápics, P. I., Tkachenko, A., Aerts, C., et al. 2015, ApJ, 803, L25
Pápics, P. I., Tkachenko, A., Van Reeth, T., et al. 2017, A&A, 598, A74
Rauer, H., Catala, C., Aerts, C., et al. 2014, Experimental Astronomy, 38, 249
Ricker, G. R., Vanderspek, R., Winn, J., et al. 2016, in Proc. SPIE, Vol. 9904, Space Telescopes and Instrumentation 2016: Optical, Infrared, and Millimeter Wave, 99042B
Rogers, T. M. 2015, ApJ, 815, L30
Rogers, T. M. & McElwaine, J. 2017, ApJ, in press
Saio, H., Kurtz, D. W., Takata, M., et al. 2015, MNRAS, 447, 3264
Schmid, V. S. & Aerts, C. 2016, A&A, 592, A116
Sowicka, P., Handler, G., Dębski, B., et al. 2017, MNRAS, 467, 4663
Tayar, J. & Pinsonneault, M. H. 2013, ApJ, 775, L1
Thompson, M. J., Christensen-Dalsgaard, J., Miesch, M. S., & Toomre, J. 2003, ARA&A, 41, 599
Townsend, R. H. D. 2003, MNRAS, 340, 1020
Triana, S. A., Moravveji, E., Pápics, P. I., et al. 2015, ApJ, 810, 16
Van Reeth, T., Tkachenko, A., & Aerts, C. 2016, A&A, 593, A120
Van Reeth, T., Tkachenko, A., Aerts, C., et al. 2015, ApJS, 218, 27
Zorec, J. & Royer, F. 2012, A&A, 537, A120
Zwintz, K., Moravveji, E., Pápics, P. I., et al. 2017, A&A, 601, A101